Received: Aug '22
Revised: Sep '22
Accepted: Sep '22

IMPLEMENTATION OF THE DEHAZING ALGORITHM IN AN EFFICIENT VIDEO DEHAZING IN BLIND TRANSMISSION MAP FUSION

Mohammad Shahbaz Khan[1] and Dr. Pramod Sharma[2]
[1]Research Scholar, University of Technology, Jaipur
[2]Professor, University of Technology, Jaipur

ABSTRACT

We look at how dehazing affects images and videos that are affected by poor atmospheric conditions. A video shot in an outdoor environment may be affected by the presence of clouds, such as haze, fog, and dust particles, in the atmosphere. To get rid of this unwelcome cloudiness from videos and constant video, we're applying a dehazing method. In order to improve the situation, we use a clever approach for video dehazing. We restore the clouded picture and video by increasing their difference because, in our opinion, they have a low degree of differentiation. This algorithm measures the transmission map to enhance the distinction of the resultant video and image after registering the air light on an informationally dim picture and video.

Single picture dehazing is frequently the subject of attention in the field of picture handling. Because improper transmission map assessment could lead to excessive difference or variety contortion in the restored images, the majority of optical dissipating models have undergone significant improvements. As a result, these dehazing algorithms are now built with consideration for transmission map assessment. In this study, we proposed a flexible single picture dehazing approach that makes use of the picture fusion method to increase the assessment precision of transmission maps. More specifically, a gamma adjustment is used largely to modify the transmission map that the dim channel got. The intricate details of the special transmission map are then maintained by integrating the weighting normal picture fusion method with the original transmission map and its modified form. The integrated transmission map is also filtered by directed channel in order to prevent brightness and block artefacts in the dehazed images. A revised transmission map produced using an optical dissipation model is then used to reconstruct the dehazed images. We evaluate the proposed method on both recent and historic murkiness photos.

Keywords: Dehazing Algorithm, Efficient Video Dehazing, Transmission Map, Fusion.

1. INTRODUCTION

Picture matching is inherently challenging when multiple images of a massive scene are being coordinated. Even though close element focuses are frequently employed to match comparable areas in different images, picture matching is challenging due to perspective, illumination, and ephemeral changes. There are two different types of photo matching strategies: include-based and region-based methods. In order to compare the similarity of the pixels between the two images, region-based techniques are used. In contrast to power values, striking aspects are simply eliminated in highlight-based tactics. Earlier remote-detecting frameworks required performing this operation physically. In any event, by using adjacent element point locators and descriptors, this cycle can now be carried out in a timely manner.

Neighborhood inclusion extraction makes use of the fundamental problems, most of which are mathematical (size, area, relative) or photometric (brightening, variety) in nature. Additionally, modern algorithms are robust and independent of changes in the image. Accordingly, these techniques are widely used in remote-detecting applications such as object recognition and identification, object tracking, scene analysis, characterisation, picture synchronisation, and recovery.

Recently, there has been growing interest in studying footage that has been affected by climatic oddities. Dehazing, or the removal of haze, is highly sought-after in consumer, computational photography, and PC vision applications. The most popular method of eradicating darkness can completely increase the scene's perceptibility and reverse the airlight's shift. Poor natural lighting conditions prevent the introduction of visual content in video. The most popular method of removing fog from video and improving video quality is dehazing, so the main goal of our strategy is to make the video more difficult to perceive, which is relevant in the fields of public safety, car crash investigation, wrongdoing criminology, remote detection region, and military

reconnaissance. The three main objectives of video improvement techniques are to examine the hidden nuances in the video; to avoid effects like shining and uneven openness; and to make the video momentarily predictable. We provide a differentiation upgrading algorithm to achieve these goals. Contrast Upgrade is frequently used for reconnaissance applications because the review environment is out of the observer's control. Startling gleams are actually eliminated by using this method. The "air light" that optical scattering causes on videos and pictures is unnecessary openness. It occurs as a result of light from the source (the sun) being scattered to reach the observer. In specified input situations, the air light is evaluated immediately away (video, image). There are several techniques for registering scene profundity, such as assessing scene profundities from at least two images and videos that were captured throughout various ecological and meteorological patterns. In order to do this, we divide an information scene into larger parts, then determine the best transmission for each block. The distinction between picture and video grew in this way. Finally, we use the gamma correction approach, which is used to optimise the use of bits while encoding images and videos. It is an effective tool for managing an image's overexposed or underexposed histogram. Gamma modification can also be naturally adapted in addition to manual control to account for scene changes. Gamma rectification in minimal video framework is done physically and with basic hardware. Gamma rectification can be provided via numerical activities in high-end hardware with computerised video framework. In order to achieve haze-free images and videos that are clearly visible to unaided eyes and have a significant impact on the clarity of the message and visual insight, we dehaze images and videos using contrast improvement algorithms from dark images and videos.

The three types of dehazing techniques currently in use are those based on past information, those based on learning, and those based on picture fusion. In earlier based approaches, the highlights of clear photos are used to analyse the transmission maps and ambient light power of the dim picture. A model based on air material science is then used to obtain the cloudy removed image. DEFADE, variety constriction earlier (CAP), dull channel earlier (DCP), variety lines, cloudiness lines, etc. are examples of common works. DCP is strongly based on the understanding that, in at least one variety channel, the forces of a hazy-free image correction are virtually nonexistent. In order to produce more accurate transmission maps, he and his colleagues proposed directed channel to update the DCP-obtained transmission map. The DCP has worked on the dehazing exhibitions from a variety of perspectives. Variety Lines are built on the fundamentals of regular images, which show a one-layered dispersion in the RGB colour space in pixels from small picture patches. The Fog Lines technique presupposes that a wide range of shades may accurately mimic an image without any fog. Due to the contrast between the beauty and the pixels' immersion in the hazy image, CAP is also a straight variety limitation. In order to acquire the transmission map more recently, a direct model that is based on ambient light evaluation is proposed. The barometrical light of each foggy image is then evaluated by the matching scene profundity map using this technique, which employs a differentiable capacity to set the bounds of a straight scene profundity model for the age of photographs.

perceptually comparable tone is discovered to be the middle value of all.

B. In 2001, Y. Y. Schechner, G. Narsimhan, and Shree K. Nayar suggested using polarisation to momentarily remove haze from a photograph. They offer a method that gets rid of the charged, ambient particle-influenced dimness from images. Through the use of a model that is affected by the polarisation effects of air dispersion, they were able to obtain the hazy image and scene structure data. Investigations into the effects of polarisation on air particles and minute residue particles lead to the capture of images through polarising channels that are placed in a plane-aligned position. They received the picture-based reach map. That employs blurrier focuses to show more momentary objects. This will become convenient for remote photography and detecting. However, this method is less effective when there is an overcast sky and when there is an exceptionally thick haze or dimness.

C. S. G. Narasimhan and Shree K. Nayar put out a Differentiation Rebuilding of Weather-Corrupted Pictures proposal in 2003. This paper presents an actual model that takes into account the persistently bad weather patterns. The main restriction to recognise profundity discontinuities in the scene is

provided by the change in capabilities of the current scene point under the terrible weather patterns. Additionally, once the scene structure has been processed, a rapid algorithm to restore scene contrast is offered. All of the techniques presented in this work are convincing in a variety of meteorological situations, such as cloudiness, haze, and fog. Additionally, dark scale, RGB tone, multispectral, and IR images can all be processed using this technique. This approach should not be used repeatedly to obtain free weather videos. This method cannot be used to reinstate the distinction between a moving object or video. This made use of an 8-cycle commercially available computerised camera.

D. Y. Y. Schechner, S. Shwartz, and E. Namer published a work on blind fog partition in 2006. The methodology for blindly recovering boundaries necessary for separating the air light from the estimation is proposed in this paper. This methodology relies on polarisation to recover the differentiation without client communication or the presence of the sky in the edge when examining murky images. It compares skyline pixels to sky pixels, and bases estimation on whether such a picture component is present in the field of vision (FOV). This tactic successfully separates the article signal from the air light without consideration for whether there is any sky in the field of view (FOV). The method makes use of numerical tools developed for Visually Impaired Source Detachment (BSS), also known as Free Part Examination (ICA), which is dependent on a range of cues.

Dehazing demonstrated a significant improvement in appearance and diversity responsive to the raw data by here using the visually handicapped boundary assessment that was consistent with direct sky estimation.

2. LITERATURE REVIEW

A. Two-sided filtering for dark and variety photographs was proposed by C. Tomasi and R. Manduchi in 1998. Through a nonlinear blending of neighbouring picture value, respectful sifting smooths out the image while protecting the edges. It combines dark degrees of variety based on their mathematical similarity and their photometric similarity, and prefers nearby values to distant ones in terms of both distance and reach. Perhaps the most important aspect of image processing and computer vision is separating. Since the components of a picture typically change gradually throughout space, it seems sense to average the pixels together since they are likely to have similar properties. An easy-to-understand non-iterative plan for edge-saving smoothing is presented in this work. It clearly allows for the requirement of any ideal photometric distance record, which is important for differentiating variety photos. It significantly increases the intrigue, which is referred to as sifting. Only variety pictures can be subjected to two-sided filtering. The CIE-lab variety space includes variations with short Euclidian distances that are clearly related to the execution of variety separation by humans. Only perceptually evident edges are protected here; only perceptually comparable tone is discovered to be the middle value of all.

B. In 2001, Y. Y. Schechner, G. Narsimhan, and Shree K. Nayar suggested using polarisation to momentarily remove haze from a photograph. They offer a method that gets rid of the charged, ambient particle-influenced dimness from images. Through the use of a model that is affected by the polarisation effects of air dispersion, they were able to obtain the hazy image and scene structure data. Investigations into the effects of polarisation on air particles and minute residue particles lead to the capture of images through polarising channels that are placed in a plane-aligned position. They received the picture-based reach map. That employs blurrier focuses to show more momentary objects. This will become convenient for remote photography and detecting. However, this method is less effective when there is an overcast sky and when there is an exceptionally thick haze or dimness.

C. S. G. Narasimhan and Shree K. Nayar put out a Differentiation Rebuilding of Weather-Corrupted Pictures proposal in 2003. This paper presents an actual model that takes into account the persistently bad weather patterns. The main restriction to recognise profundity discontinuities in the scene is provided by the change in capabilities of the current scene point under the terrible weather patterns. Additionally, once the scene structure has been processed, a rapid algorithm to restore scene contrast is offered. All of the techniques presented in this work are convincing in a variety of meteorological situations, such as cloudiness, haze, and fog. Additionally, dark scale, RGB tone, multispectral, and IR images can all be processed using this technique. This approach should not be

used repeatedly to obtain free weather videos. This method cannot be used to reinstate the distinction between a moving object or video. This made use of an 8-cycle commercially available computerised camera.

D. Y. Y. Schechner, S. Shwartz, and E. Namer published a work on blind fog partition in 2006. The methodology for blindly recovering boundaries necessary for separating the air light from the estimation is proposed in this paper. This methodology relies on polarisation to recover the differentiation without client communication or the presence of the sky in the edge when examining murky images. It compares skyline pixels to sky pixels, and bases estimation on whether such a picture component is present in the field of vision (FOV). This tactic successfully separates the article signal from the air light without consideration for whether there is any sky in the field of view (FOV). The method makes use of numerical tools developed for Visually Impaired Source Detachment (BSS), also known as Free Part Examination (ICA), which is dependent on a range of cues.

Dehazing demonstrated a significant improvement in appearance and diversity responsive to the raw data by here using the visually handicapped boundary assessment that was consistent with direct sky estimation.

3. VIDEO DEHAZING

We use the latest techniques into our video dehazing technology. Figure 3 shows the stream outline of our system.

The fuzzy video's primary imaging model is provided by

$$I(x,s) = t(x,s)J(x,s) + (1-t(x,s))A, \quad (1)$$

where x is the size of a single pixel in an outline s, I is the hazy video, J is the brightness of the scene on a clear morning, t is the medium transmission, which represents the portion of light that isn't scattered and reaches the camera, and An is the range of environmental conditions around the world. Recovering t(x,s), J(x,s), and A for every pixel x in each case s is the goal of picture reclamation.

We anticipate that the barometric variety A will be constant during the whole video, making measurement easy. The majority of photo dehazing algorithms calculate A using the pixels with the strongest forces, which is speedy but unreliable. For instance, a white building or car might have the most bright pixel. He et al .'s coordination of the airlight evaluation with the earlier dim channel results in a more precise assessment outcome. Here, we modify the method he suggested.

We continue with the supplementary steps to restore the perceivability of the foggy picture in light of the barometric variety A.

3.1. Frame-by-frame dehazing

We initially obtain the rough transmission map for each frame s utilising the dark channel previous,

$$\tilde{t}(\mathbf{x},s) = 1 - \omega \min_{c\in r,g,b}\left(\min_{\mathbf{y}\in\Omega(\mathbf{x})}\left(\frac{\mathbf{I}^c(\mathbf{y})}{\mathbf{A}^c}\right)\right),$$

Where the boundary is used to save a small amount of fog for distant objects, which is useful in some situations. The is fixed at 0.95 as stated in the proposal.

Then, to improve the rough transmission map t, we consolidate the directed channel algorithm (x,s). The revised transmission map T(x,s) is anticipated to be a direct alteration of the foggy(guidance) picture I(x,s) in a window (x) focused at pixel x for each edges

3.2. Optical flow estimation

$$\hat{t}(\mathbf{y},s) = \mathbf{a}_x^{\mathrm{T}}\mathbf{I}(\mathbf{y},s) + b_x, \forall \mathbf{y} \in \omega_x,$$

A video succession's individual pixels can be evaluated for interframe movement using an optical stream technique. The most fundamental assumption in optical stream estimation is picture splendour steadiness for two adjacent outlines, I(x,s) and I(x,s + 1). Because of the variance from top to bottom in a hazy picture pair, the brilliance of the corresponding pixels isn't exactly equal to one another. Fortunately, a video shows that the difference between two adjacent edges is incredibly small. We acknowledge that the splendour restriction is also valid.

$$\mathbf{I}(\mathbf{x},s) \approx \mathbf{I}(\mathbf{x}+\mathbf{u},s+1),$$

where u is the pixel's speed. We pre-sift as suggested in order to reduce the magnificence difference between two casings. Sun's most recent optical stream assessment algorithm, whose execution is available on the creator's website page, was combined with our video dehazing technique.

We use the method suggested in to make the most of optical stream to its best possible benefit. We identify two different types of stream fields for each case s, such as the forward stream u f s from outline s 1 to approach s and the reverse stream u b s from

outline s+1 to approach s. We create the forward error map M f s and the backward error map Mb s to determine the accuracy of these two stream fields. The corresponding pixels for a pixel in an outline are x in outline s, x in outline s 1, and x in outline s + 1, respectively. In RGB variety space, we calculate the contrast between the expected variety and the observed variety.

$$M_s^f = ||I(\mathbf{x},s) - I(\mathbf{x}-\mathbf{u}_s^f, s-1)||_2$$
$$M_s^b = ||I(\mathbf{x},s) - I(\mathbf{x}-\mathbf{u}_s^b, s+1)||_2$$

Where || • ||2 denotes a vector's L2 standard. The error maps, both forward and backward, provide us with an action at each pixel of the accuracy of stream assessment from the prior and succeeding casings. Figure 5 displays the mistake maps. We use this information to build the MRF and work on the transient intelligence.

3.3. Temporal coherence improvement

We continue with a statically smoothing along the fleeting aspect using MRF to work on the spatial and worldly soundness of t (x,s), which is driven by, with the suspicion that the transmissions of the related pixels differ without a hitch.

The 3D MRF model exhibits the following properties for a murky video with n outlines,

$$P(t) \propto \prod_{s=1}^{n} \prod_{\mathbf{x}\in\mathbf{I}(\mathbf{x},s)} \exp(-(t(\mathbf{x},s) - \hat{t}(\mathbf{x},s))^2/\sigma_p^2) \cdot \prod_{\forall \mathbf{y}\in\Omega_x} \exp(-P_s(\mathbf{x},\mathbf{y},s)\cdot(t(\mathbf{x},s) - t(\mathbf{y},s))^2/\sigma_s^2) \cdot \prod_{\forall c\in\{f,b\}} \exp(-P_t(\mathbf{x},c,s)\cdot(t(\mathbf{x},s) - t(\mathbf{x}-\mathbf{u}_s^c, s'))^2/\sigma_t^2)$$

4. THE PROPOSED METHOD

Fig. 1 shows the broad layout of the suggested technique. The initial transmission map is chosen in consideration of DCP and revised by gamma modification. Through the picture fusion approach, the underlying transmission map and its rectified form are combined. The combined transmission map is then sorted by directed channel at that point. Finally, using an optical dissipation model and the obtained transmission map, the dehazed images are recovered.

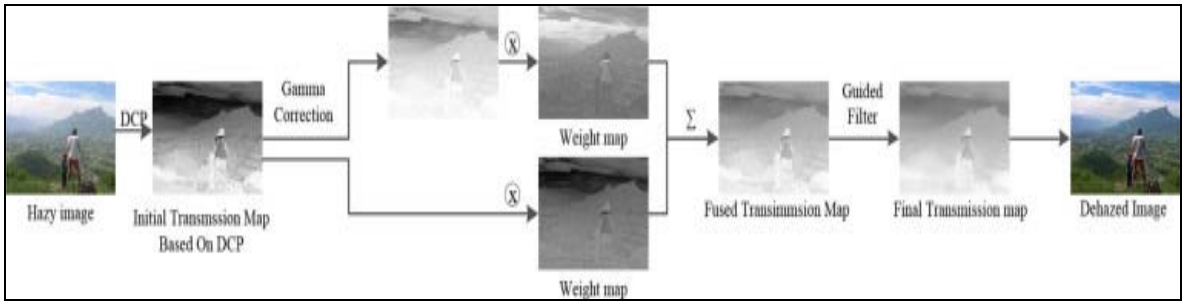

Figure: 1. a visual representation of the suggested method's flowchart.

4.1. Transmission map via gamma correction

The transmission map with Gamma correction formula is defined as follows

$$T_2(x) = T_1(x)^{\frac{1}{\lambda}}$$

where T1(x) is derived from the recipe, and x is the pixel facilitates. Two bends with =1 and 4 independently are shown in Fig. 2. When the value is equal to 4, the distinctive reach increases in the low dim worth region and the picture contrast is enhanced, but the powerful reach reduces in the high dim worth region and the picture contrast is decreased.

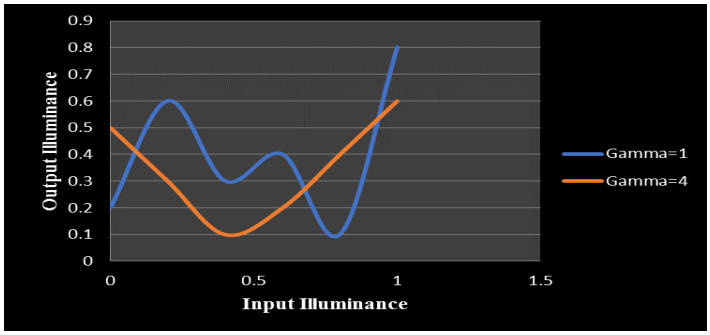

Figure: 2. The Gamma correction curve

4.2. Adaptive image fusion for transmission map estimation

The accuracy of the transmission map assessment is worked on adaptively using the weighting normal picture fusion technology. Murky images often include two types of regions: heavily clouded regions and less foggy ones. The transmission map as evaluated by DCP is excellent in areas with heavy fog. Consequently, giving the original transmission map more weight and the Gamma revision less weight. In any event, the transmission map evaluated by DCP is consistently inaccurate in less cloudy regions. As a result, the transmission managed by Gamma remedy is given more weight, but the transmission obtained by DCP is given less weight. As a result, the fusion dish can be described as.

$$T_F(x) = T_1(x) W_F(x) + T_2(x)(1 - W_F(x))$$

where the individual maps T1(x) and T2(x) represent the underlying transmission map and its Gamma remedy map. The estimation stream graph of WF(x), the fusion weighting.

The underlying transmission map and its gamma adjustment map are sorted based on directed channel as from the beginning.

$$G_1(x) = GuidF_{\tau,\varepsilon}(T_1(x))$$

and.

$$G_2(x) = GuidF_{\tau,\varepsilon}(T_2(x))$$

GuidF, (•) addresses directed channel with boundaries "and" in that case. As the aid maps, T1(x) and T2(x) are sorted together.

The development of weighting happens after that.

$$W_F(x) = \frac{T_1(x)T_2(x)}{(G_1(x)+a)(G_2(x)+a)}$$

Which guarantees the preservation of the transmission map's details? A is a variable whose value is determined by.

$$a = \frac{\max(I^{dark}(x))}{k}$$

When k is a constant The cloudy photos determine versatile weighting maps, therefore the suggested method reestablishes numerous cloudy pictures in an adaptive manner.

Then, a channel-directed fused transmission map is completed to achieve a superior presentation with obvious impact, which can address the radiance issue and block remnants of the dehazed picture.

$$T_F(x) = GuidF_{\tau,\varepsilon}(I^{gray}(x), T_F(x))$$

I

gray(x) represents the grey, or guided, map, of the original image. The dehazed image is then obtained.

$$J(x) = \frac{I(x)-A}{T_F(x)} + A$$

5. EXPERIMENTAL RESULTS

This section focuses mostly on the establishment of free boundaries. The displays of the suggested strategy and eight old-style or modern examination techniques—specifically, He et al., Zhu et al., Berman et al., Cai et al., Dhara et al., Zheng et al., Zhu et al., and Ju et al.—are then subjected to broad analyses to evaluate. To continue the experiments, six typical foggy images that include dense dim and less dim, murky at near and far distances, are picked. Five cloudy manufactured images from the generally accessible dataset Dwell are also chosen to further approve the analyses.

5.1. Parameter settings

On a computer with an Intel(R) Center (TM) i7-10875UCPU@ 2.30 GHz 16.00 GB Smash, the trials were run in MATLAB2018b. In, the boundaries between and are experimentally set at 15 and 0.001, respectively, with a basic separation patch size of 5 5. In both the PSNR and SSIM objective pointers that have been proposed, gamma in and k in play a key role. As a result, we conducted a number of researches to look at the acceptable border values.

5.2. Subjective comparison on natural images and synthetic images

The issue of variety contortion and over-upgrading in certain places is present in the outcome photographs, as is evident in N3, N5, S1, S3, and S4. Similitude, the dehazed results of the Berman et al. technique were over-upgraded due to the

incorrect transmission map assessment for several images, as seen in N3, N4, and N5. In light of He et altechnique,'s Dhara et al. offered a variety solution that can effectively address the problem of variety contortion. Consequently, Dhara et alimproved.'s technique for visualising dehazed images is effective. The picture update is necessary for both the Zheng et al. technique and the Zhu et al. technique. Despite their excellent dehazing performance, the variety relics increase as a result, and as a result, the dehazed outcomes heavily rely on the better photos, as can be seen in N1, N3, N4, and S1. The Ju et al. strategy's dehazed effects clearly indicate over-easing up. This is due to the climate dispersing model's (ASM) presentation of a light retention coefficient, which might improve the overall magnificence of outcomes. In general, the techniques developed by Zhu et al., Cai et al., and the proposed strategy may effectively remove darkness in source images. The colour of the restored images is also consistent and logical.

5.3. Quantitative comparisons

Given that different viewers would react differently, objective markers are trained to evaluate the demonstrations of various strategies statistically. These metrics include the principal likeness percentage (SSIM), the top sign-to-clamor ratio (PSNR), and the normal picture quality evaluator (NIQE). The NIQE is a non-reference marker at that time. The more modest the NIQE, the more realistic and typical the restored images are. Both the Zheng et al. and the Zhu et al. techniques have significant NIQEs since their dehazed findings show obvious variety bending. The dehazed effects of the He et al., Berman et al., and Ju et al. techniques have been over-upgraded. Their typical NIQE is therefore moderately high. Since the dehazed images produced by Zhu et al. approach, Dhara et al. strategy, and the suggested technique are usually reasonable, they can all obtain moderately low NIQE.

6. CONCLUSION

An algorithm called "Difference Enhancement" is suggested after looking at how video and picture are affected by unusual weather and other natural circumstances (just fog). The process of contrast improvement uses the options available on the presentation or outcome device to make the video and picture highlights stand out more clearly. This algorithm is applied to images and videos before moving on to ongoing video, which can be used in a framework for reconnaissance in the area of public security. The air light can be used to determine the video and picture quality. The profundity assessment technique is then applied to identify the given input's profundity data. Finally, gamma treatment is used to remove the visual discerning quality from images and videos.

We assessed the transmission map using image fusion and proposed a successful single picture dehazing method. This strategy depends on the DCP, which has areas in which it excels, to carry out dehazing effectively. With the goal of maintaining our superior dehazing performance, we want to solve the issue of excessive improvement and variety bending in DCP. As a result, we first use Gamma rectification to pre-process the transmission map produced by DCP. Then, we recommend an adaptively fusion system to fuse the pre-handled picture with the underlying transmission picture obtained by DCP. The adaptive fusion method, which also permits varying degrees of image obscurity, can preserve the subtleties in restored images. Finally, we deal with the corona problem and reduce the influence of sky districts by managing an interlaced transmission map via a directed channel. We analyse the presentation of picture reproduction using NIQE, PSNR, and SSIM, and compare our method to eight state-of-the-art techniques in both modern and historical cloudiness photos. In the interim, computation time is also investigated. The findings show that our method is effective in addressing the problem of excessive upgrades and variety mutilation of recovered images, and that it estimates images considerably more quickly than DCP does. Future development will concentrate on picture dehazing's thick dim implementation. Wanting to do dehazing in a very overcast environment and produce amazing outcomes in both.

REFERENCES

1. Al Zorgani, M. and Ugail, H., 2018. Comparative Study of Image Classification using Machine Learning Algorithms (No. 332). EasyChair.
2. Al-dahoud, A. and Ugail, H., 2017. A method for location based search for enhancing facial feature detection. In Advances in

Computational Intelligence Systems (pp. 421-432). Springer, Cham.
3. Chen, Y.; Xu, W.; Piao, Y. Target matching recognition for satellite image based on the improved FREAK algorithm. Math. Probl. Eng. 2016, 2016, 1–9.
4. Elmahmudi, A. and Ugail, H., 2019. Deep face recognition using imperfect facial data. Future Generation Computer Systems, 99, pp.213-225.
5. Farooq, J. Object detection and identification using SURF and BoW model. In Proceedings of the 2016 International Conference on Computing, Electronic and Electrical Engineering (ICE Cube), Quetta, Pakistan, 11–12 April 2016.
6. Feng Yu, Chunmei Qing, Xiangmin, Xu, Bolun Cai, "Image and video dehazing using view-based cluster segmentation", 2016.
7. Halavataya, K. Local feature descriptor indexing for image matching and object detection in real-time applications. Pattern Recognit. Image Anal. 2020, 30, 16–21.
8. Hassan, S.I., Dang, L.M., Mehmood, I., Im, S., Choi, C., Kang, J., Park, Y.S. and Moon, H., 2019. Underground sewer pipe condition assessment based on convolutional neural networks. Automation in Construction, 106, p.102849.
9. Jin-Hwan Kim, J-Y Sim, X. Tang, "Single image dehazing based on contrast enhancement", IEEE, International Conference on Acouatics, vol. 7882, no. 1, pp. 1273-1276, 2011.
10. Leng, C.; Zhang, H.; Li, B.; Cai, G.; Pei, Z.; He, L. Local feature descriptor for image matching: A survey. IEEE Access 2019, 7, 6424–6434.
11. M. Gopika, M. Sirisha, "Visibility Enhancement of hazy image using Depth Estimation Concept", IRJET, vol. 4, Issue. 7, pp. 3300- 3305, July 2017
12. Rani, R.; Grewal, S.K.; Panwar, K. Object recognition: Performance evaluation using SIFT and SURF. Int. J. Comput. Appl. 2013, 75, 39–47.
13. S. Salazar-Colores, E. Cabal-Yepez, J.M. Ramos-Arreguin, et al. A fast image dehazing algorithm using morphological reconstruction IEEE Trans. Image Process., 28 (5) (2018), pp. 2357-2366
14. Shao, Y.; Li, L ; Ren, W.; et al.; Domain adaptation for image dehazing. Proc. IEEE Conf Comput. Vis. Pattern Recognit.(CVPR)., 2020: 2808-2817.
15. Tuytelaars, T.; Mikolajczyk, K. Local invariant feature detectors: Survey. Found. Trends Comput. Graph. Vis. 2008, 3, 177–280.
16. Ugail, Hassan, and Ahmad Al-dahoud. "A genuine smile is indeed in the eyes–The computer aided non-invasive analysis of the exact weight distribution of human smiles across the face." Advanced Engineering Informatics 42 (2019): 100967.
17. Xi, W.; Shi, Z.; Li, D. Comparisons of feature extraction algorithm based on unmanned aerial vehicle image. Open Phys. 2017, 15, 472–478.
18. Yongmin Park, Tae-Hwan kim, "Fast execution scheme for dark-channel-prior outdoor video dehazing", IEEE, ACCESS, vol. 6, pp. 10003-10014, March 2018.
19. Zhang, C.-M.; Gong, Z.-H.; Huang, Y. Performance evaluation and improvement of several feature point detectors. J. Geomat. Sci. Technol. 2008, 25, 231–234.
20. Zhou, H.; Dai, A.; Tian, T.; Tian, Y.; Yu, Z.; Wu, Y.; Zhang, Y. Feature matching for remote sensing image registration via manifold regularization. IEEE J. Sel. Top. Appl. Earth Obs. Remote. Sens. 2020, 13, 4564–4574.